

REPORT DOCUMENTATION PAGE

*Form Approved
OMB No. 0704-0188*

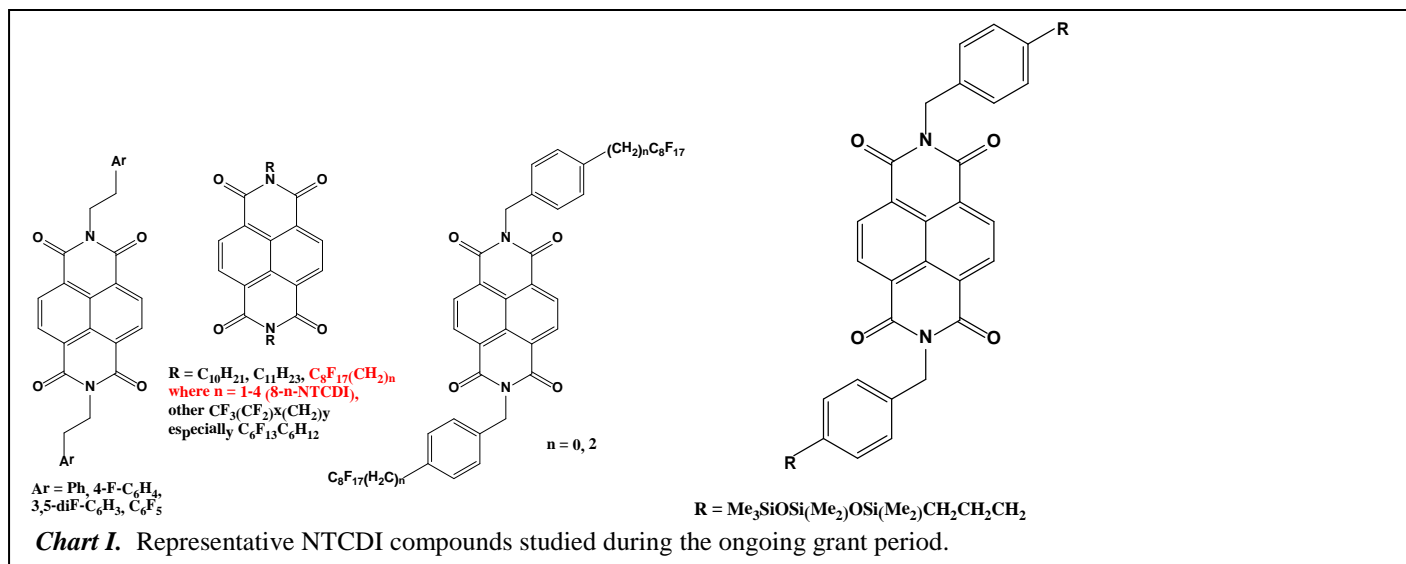
The public reporting burden for this collection of information is estimated to average 1 hour per response, including the time for reviewing instructions, searching existing data sources, gathering and maintaining the data needed, and completing and reviewing the collection of information. Send comments regarding this burden estimate or any other aspect of this collection of information, including suggestions for reducing the burden, to the Department of Defense, Executive Services and Communications Directorate (0704-0188). Respondents should be aware that notwithstanding any other provision of law, no person shall be subject to any penalty for failing to comply with a collection of information if it does not display a currently valid OMB control number.

PLEASE DO NOT RETURN YOUR FORM TO THE ABOVE ORGANIZATION.

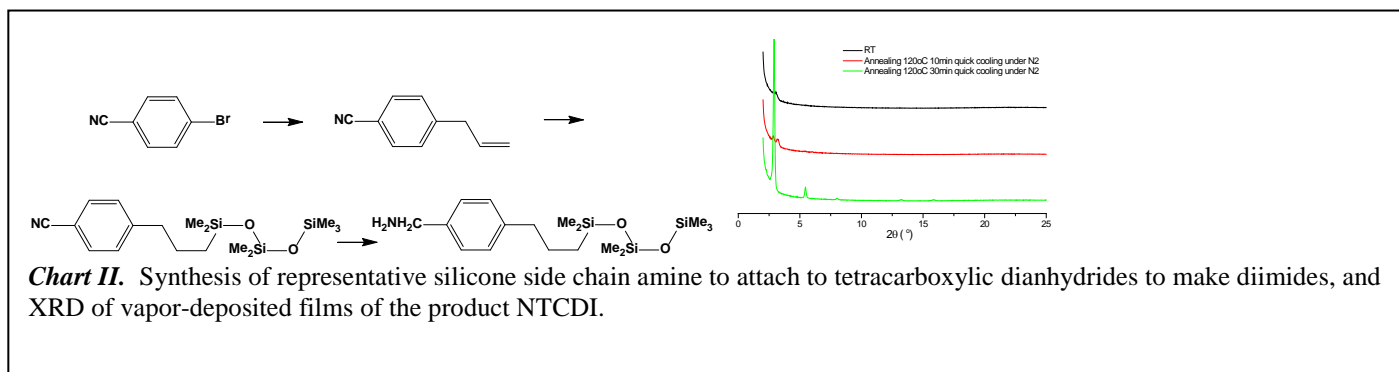
1. REPORT DATE (DD-MM-YYYY)		2. REPORT TYPE		3. DATES COVERED (From - To)	
4. TITLE AND SUBTITLE				5a. CONTRACT NUMBER	
				5b. GRANT NUMBER	
				5c. PROGRAM ELEMENT NUMBER	
6. AUTHOR(S)				5d. PROJECT NUMBER	
				5e. TASK NUMBER	
				5f. WORK UNIT NUMBER	
7. PERFORMING ORGANIZATION NAME(S) AND ADDRESS(ES)				8. PERFORMING ORGANIZATION REPORT NUMBER	
9. SPONSORING/MONITORING AGENCY NAME(S) AND ADDRESS(ES)				10. SPONSOR/MONITOR'S ACRONYM(S)	
				11. SPONSOR/MONITOR'S REPORT NUMBER(S)	
12. DISTRIBUTION/AVAILABILITY STATEMENT					
13. SUPPLEMENTARY NOTES					
14. ABSTRACT					
15. SUBJECT TERMS					
16. SECURITY CLASSIFICATION OF:			17. LIMITATION OF ABSTRACT	18. NUMBER OF PAGES	19a. NAME OF RESPONSIBLE PERSON
a. REPORT	b. ABSTRACT	c. THIS PAGE			19b. TELEPHONE NUMBER (Include area code)

List of Completed and Published Tasks, 2009-2012

1. Synthesis of new naphthalenetetracarboxylic diimide (NTCDI) compounds. During 2009-12, NTCDIs with alkyl, perfluoroalkyl, perfluorophenylalkyl, and silicone side chains were prepared, as shown in Charts I and II. The fluorinated side chains lead to excellent OSCs. The silicone side chains self-organize from solution, as shown by XRD, but with little OFET activity. An especially bulky and hydrophobic side chain, 2-decalinylmethyl, was synthesized in stereopure form for the first time.



2. Measurement of μ , effective sheet transconductance, dielectric constant, and dielectric strength. This was

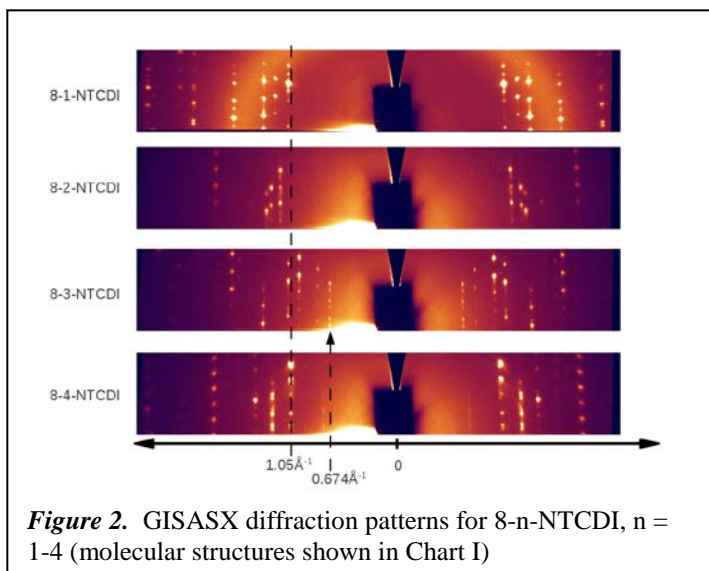
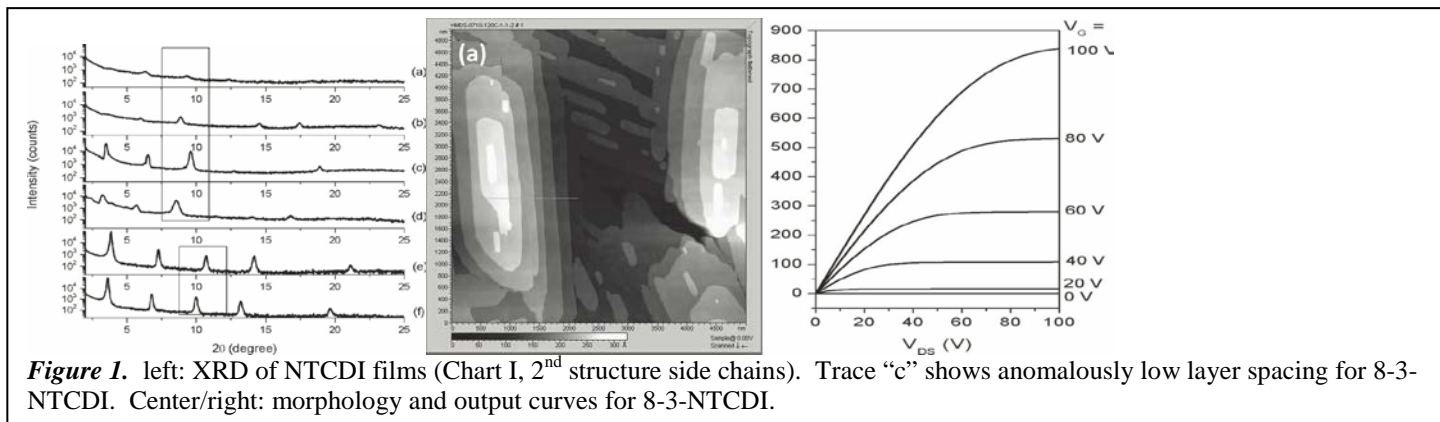


accomplished for a series of perfluoroalkylalkyl and perfluoroalkylbenzyl compounds, with focus on one particular promising molecule. There was an anomalously high μ , $>0.6 \text{ cm}^2/\text{Vs}$, in conventional OFETs from the perfluoro-octylpropyl NTCDI (8-3-NTCDI, see red substituent label in Chart I) relative to perfluoro-octylmethyl, -ethyl, and -butyl NTCDIs. (Jung and Lee, 2010) This μ was related to unusually high interaction energy, large area grains, and differentiated thin film phase revealed by standard x-ray diffraction (XRD) for the molecule, and was accompanied by air-operability and low hysteresis. Key data are shown in Figure 1. The compound also showed μ of $0.05 \text{ cm}^2/\text{Vs}$ on a high-capacitance ionically polarizable oxide dielectric. (Pal and Dhar, 2009) Also, a gold-parylene layer provides passive but highly beneficial stabilizing function to bis(pentafluorophenethyl)NTCDI. The device had alumina gate dielectric, and the capacitance times mobility was 80 nS/V (10x typical pentacene/oxide), stable to heating to 70°C in air.

Remarkably, specular x-ray diffraction performed by Kevin Evans-Lutterodt at Brookhaven National Laboratories confirmed much more definitively that 8-3-NTCDI has a different thin film crystal structure, with strong reflections from features spaced farther apart, than the other three compounds. Using the configuration typical for Grazing Incidence Small Angle X-ray Scattering (GISAXS) XRD measurements were carried out at Beamline X13B at the National Synchrotron Light Source. The in-vacuum undulator was set at minimum gap to give a peak photon flux at photon energy 11.45 keV. The incident angle of the beam with respect to the film surface was adjusted to be below the critical angle. A Kirkpatrick-Baez mirror pair focused the beam to a

beamsize of order 5 microns. This keeps the beam restricted to the surface area of the film, thus enhancing the signal to noise.

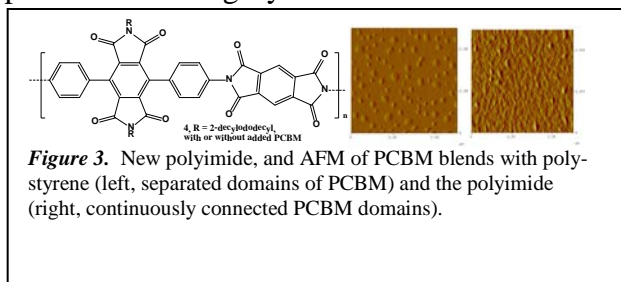
A Princeton Instruments CCD area detector was placed 142 mm downstream of the sample. The CCD images were 2084x2084 pixels, with a pixel spacing of 55 μm . Distance from sample to detector was calibrated using a NIST standard Al_2O_3 powder. The diffraction patterns for the compounds 8-1-NTCDI through 8-4-NTCDI are arranged in the four panels of Figure 2, from top to bottom respectively. As can be seen from the diffraction spots in Figure 2, all the compounds form ordered films, but the crystal structures are different for each film. For homologous series like for the series studied here, one generally finds that the crystal structures and hence the diffraction patterns to be similar across the series except for expansions or contractions, which would



correspond to a simple scaling of the measured diffraction patterns. Here, each structure appears quite different, with 8-3 NTCDI particularly unique. Figure 2 suggests the unit cell size as a differentiating factor. For 8-4, 8-2, and 8-1, the smallest q vector is of order 1.05 \AA^{-1} , which corresponds to the largest layer spacing of order 5.98 \AA , and this is indicated by the dashed line that spans the four panels. However 8-3 has an even smaller q vector indicated by the arrow, 0.674 \AA^{-1} , which corresponds to a layer spacing of 9.25 \AA . A preliminary analysis suggests that the unit cell in the plane is 9.25 \AA by 6.33 \AA with a 53.5 degree angle between the axes. A more detailed analysis that will clarify the arrangement of the molecules within the unit cell is underway.

3. Synthesis of NTCDIs with two or more side chain segments. The perfluoroalkylalkyl and silicone NTCDIs synthesized are in this category. For example, the pefluorohexylhexyl side chain, shown in Chart I, gave μ of $0.09 \text{ cm}^2/\text{Vs}$ in air.

4. Use of the new side chains on other cores. The new side chains are being applied to pyromellitic diimide (PyDI) cores, rather than perylenetetracarboxylic diimide (PTCDI) cores, because of the interest in hybrid OSC-dielectric function and low leakage current, combined with transparency and ease of processing. Short p-cores are being synthesized with these side chains. Long side chains are also being used on PyDI



polymers which will combine the functions of dielectric polyimides and self-organized n-channel OSCs.

The first polyimide, a class of polymers generally considered an insulator before this work, was made. (Kola and Tremblay, 2012) The structure shown in Figure 3 has FET mobility of $0.0001 \text{ cm}^2/\text{Vs}$ in a bottom-gate geometry. While this value is modest, there are numerous

opportunities for improvement: making the structure planar, decreasing the size of the alkyl groups, using top gate architecture, and inserting charge injection layers under electrodes. The polyimide, the first combining C and N linkages, uses less expensive starting materials, and is more soluble, stable, and transparent. The polymer was also blended with PCBM, obtaining mobility of $0.003 \text{ cm}^2/\text{Vs}$, which was increased to $>0.01 \text{ cm}^2/\text{Vs}$ on exposure to amine, suggesting that adding amine functionality to the composite will also increase mobility. AFM analysis shows particular compatibility between the polyimide and PCBM, compared to using polystyrene as a binder.

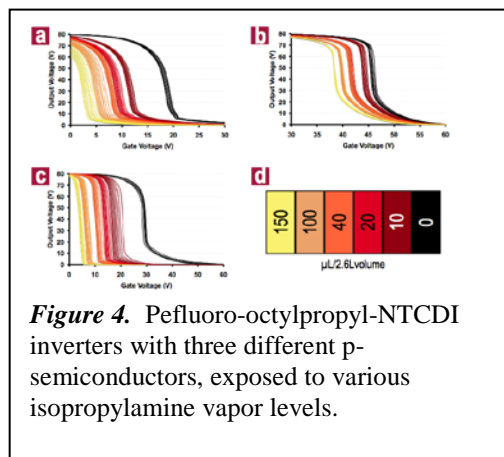


Figure 4. Pefluoro-octylpropyl-NTCDI inverters with three different p-semiconductors, exposed to various isopropylamine vapor levels.

5. Testing new materials in circuits and sensors. *N,N'*-bis(perfluorooctylbenzyl)NTCDI showed decreased I_d in response to dinitrotoluene vapor. Perfluoropropyl-NTCDI, synthesized as part of task 1, was employed in inverters (Figure 4) that had gains >50 , and that were sensitive to medically relevant amine vapors. Amine concentrations could be read directly from shifts in switching voltage. I_d and μ increased in the NTCDI arms of the inverters during exposure to amines. (Tremblay 2011)

6. Testing in energy conversion applications. An NTCDI multilayer study included a detailed examination of capacitance. The absolute low frequency capacitance was $>600 \text{ nF/cm}^2$. Up to two volts was applied without breakdown. With one volt applied, the energy stored was $>300 \text{ nJ/cm}^2$. The thickness of the dielectric giving this capacitance was $<6 \text{ nm}$ ($6 \times 10^{-7} \text{ cm}$, giving a dielectric strength of up to 3 MV/cm), so the energy density was $>0.5 \text{ J/cm}^3$. Though coming from a flat, nonelectrolytic device, this value is only two orders of magnitude less than that of a state-of-the-art high-surface-area supercapacitor.

7. Radiation stability testing of new films and devices. The perfluoro-octylbenzyl NTCDI OFET (7 monolayers) on native oxide was stable to 100 krad exposure (Figure 5). This is equivalent to one month geostationary earth orbit (GEO) or 1-2 years in low earth orbit (LEO). Even after ten times this exposure, the OFET still showed transfer activity, though V_t was shifted. More detailed studies are in progress.

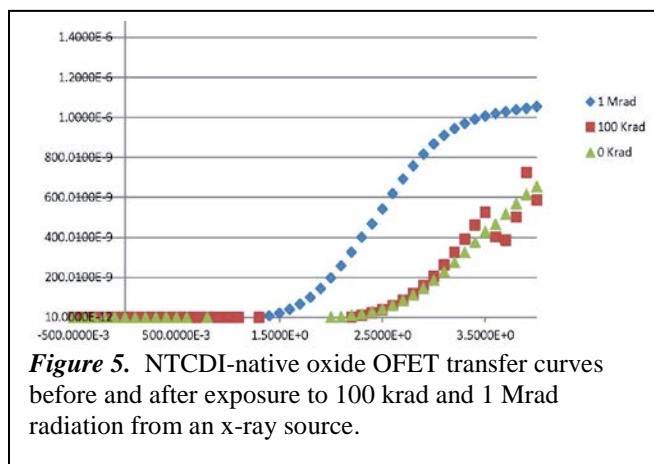


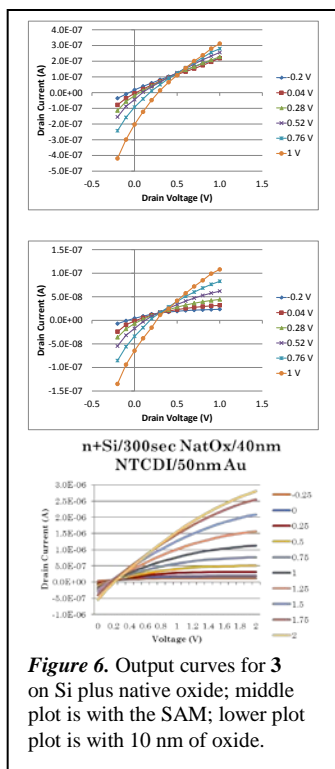
Figure 5. NTCDI-native oxide OFET transfer curves before and after exposure to 100 krad and 1 Mrad radiation from an x-ray source.

During the past three years, fourteen manuscripts were published acknowledging support of the Katz AFOSR program, listed in the “bibliography”. In addition, graduate student Bal Mukund Dhar received his Ph.D. with primary support from the program, and is now a postdoctoral fellow at NIST. Graduate student Josue

Martinez Hardigree, initially supported by the AFOSR program, completed all requirements prior to thesis, is fully trained in the techniques of the proposal, and was awarded an NSF Predoctoral Fellowship. Two additional graduate students have joined the program.

Additional Completed Work, 2011-2012

We increased FET on/off ratio where there is virtually no gate dielectric by using a dipolar self-assembled monolayer (SAM). Eliminating the gate dielectric will decrease trap states and radiation absorption cross section, increasing mobility and cosmic radiation stability. With insulating side chains on NTCDIs and other organic semiconductors (OSCs), the channel can be farther from the gate electrode, where the mobility is higher. We insert the SAM between gate electrode native oxide and the OSC. The dipole field creates a barrier to leakage in the direction of gate injection of majority carriers, corresponding to the “off” state, lowering off current and increasing on/off ratio. This dipole can even turn a nearly pure resistor into a transistor. The voltage inserted by the SAM was directly visualized using a scanning probe technique, and this voltage agreed with threshold voltage shifts recorded in transistor studies. Figure 6 shows output curves of two transistors with only a native oxide (2-3 nm) on a Si gate and 40 nm of **3** as OSC. Voltages were pulsed and currents recorded at 1 kHz. The thick film and unpatterned gate result in high leakage currents; the upper plots hardly



show any switching. However, the middle plots, from a device with a 1H,1H,2H,2H-perfluorooctylsilyl monolayer on the oxide, begin to show transistor switching. A nonfluorinated silane, with a lower dipole moment, had much less of an effect. The leakage current is further reduced, and good switching obtained, with just 10 nm of oxide, as shown in the lower plots. Capacitance times mobility was about 50 nS/V. The thin oxide enables operation <1 V, saving power. Pulsing increases effective mobility in 3 and other OSCs by as much as a factor of 4, showing that many literature mobilities, and therefore operational speeds, may be higher than realized if they were originally based on 1kHz capacitances I-V characteristics measured with direct current.

Bibliography of Publications Supported by this Grant

Pal, B.N.; Trottman, P.; Sun, J.; Katz, H.E.

“Solution-deposited Zinc oxide and Zinc oxide/Pentacene Bilayer Transistors: High Mobility n-Channel, Ambipolar and Nonvolatile Devices” *Adv. Funct. Mater.* 18, 1832-1839 (2008)

Sun, J.; Pal, B.N.; Jung, B.J.; Katz, H.E.

“Solution-processed hybrid p-n junction vertical diode” *Organic Electronics*, 10, 1-7 (2009)

Jung, B.-J.; Sun, J.; Lee, T.; Sarjeant, A.; Katz, H.E.

“Low Temperature-processible, Transparent, and Air-operable n-channel Fluorinated Phenylethylated Naphthalenetetracarboxylic Diimide Semiconductors Applied to Flexible Transistors” *Chemistry of Materials*, 21, 94-101 (2009)

Lee, T.; Landis, C.L.; Dhar, B.M.; Jung, B.J.; Sun, J., Sarjeant, A.; Lee, J.-J.; Katz, H.E.

“Synthesis, Structural Characterization, and Unusual Field-Effect Behavior of Organic Transistor Semiconductor Oligomers: Inferiority of Oxadiazole Compared with Other Electron-Withdrawing Subunits” *J. Am. Chem. Soc.*, 131, 1692-1705 (2009)

Sun, J.; Devine, R.; Dhar, B.M.; Jung, B.J.; See, K.C.; Katz, H.E.

“Improved Morphology and Performance from Surface Treatments of Naphthalenetetracarboxylic Diimide Bottom Contact Field Effect Transistors” *ACS Applied Materials and Interfaces* 1, 1763-1769 (2009)

Pal, B.N.; Dhar, B.M.; See, K.C.; Katz, H.E.

“Solution-Processed High Capacitance Transparent Sodium beta-Alumina Film: Application to Low Voltage Field Effect Transistors” *Nature Materials*, 8, 898-203 (2009)

Zheng, Q.; Jung, B.J.; Sun, J.; Katz, H.E.

“Ladder-Type Oligo-*p*-Phenylene-Containing Copolymers with High Open-Circuit Voltages and Ambient Photovoltaic Activity” (cover article) *J. Am. Chem. Soc.* 132, **5394-5404** (2010)

Dhar, B.M.; Kini, G.; Xia, G.; Jung, B.J.; Markovic, N.; Katz, H.E.

“Field-effect Tuned Lateral Organic Diodes”, *Proc. Nat. Acad. Sci.*, 107, 3972-3976 (2010)

See, K.C.; Katz, H.E. “Naphthalenetetracarboxylic Diimides as Transparent Organic Semiconductors” (invited) in “Transparent Electronics: From Synthesis to Applications”, Facchetti, A. and Marks, T.J., eds. Wiley & Sons, 2010

Jung, B.J.; Lee, K.; Sun, J.; Andreou, A.G.; Katz, H.E.

“Air-operable, High-mobility Organic Transistors with Unsubstituted Naphthalenetetracarboxylic Diimide Cores: Environmental and Bias Stress Stability”

Adv. Funct. Mater., 20, 2930-2944 (2010)

Jung, B.-J.; Tremblay, N.J.; Yeh, M.-L.; Katz, H.E.

“Molecular Design and Synthetic Approaches to Electron-transporting Organic Transistor Semiconductors” (invited) Chemistry of Materials, 23, 568-582 (2011)

Jung, B.J.; Martinez Hardigree J.F.; Dhar, B.M.; Dawidczyk, T.J.; Sun, J.; See, K.C.; Katz, H.E.

“Naphthalenetetracarboxylic Diimide Layer-based Transistors with Nanometer Oxide and Side Chain Dielectrics Operating below One Volt” ACS Nano, 5, 2723-2734 (2011)

Tremblay, N.J.; Jung, B.J.; Breysse, P.; Katz, H.E. “Digital Inverter Amine Sensing via Synergistic Responses by n and p Organic Semiconductors” Adv. Funct. Mat. 21, 4314-4319 (2011)

Kola, S.; Sinha, J.; Katz, H.E. “Organic Transistors in the New Decade: Toward N-Channel, Printed, and Stabilized Devices” (invited review) J. Pol. Sci., Pol. Phys. DOI: 0.1002/polb.23054 (2012)

Kola, S.; Tremblay, N.J.; Yeh, M.-L.; Katz, H.E.; Kirschner, S.B.; Reich, D.H. “Synthesis and Characterization of a Pyromellitic Diimide-Based Polymer with C- and N-Main Chain links: Matrix for Solution-Processable n-Channel Field-effect Transistors” ACS Macro Lett. dx.doi.org/10.1021/mz200007p (2012)

Additional Detail on Completed Work

n-OFETs with minimal gate oxide and side chain dielectrics. An n-channel N,N'-bis(4-perfluorooctylbenzyl) naphthalenetetracarboxylic diimide (8-0-Bn-NTCDI) OFET (Figure 1) on a silicon gate with only 2-3 nm of native oxide as the initial gate dielectric was comprehensively analyzed.¹ The lamellar, densely packed side chains also showed dielectric activity, and contributed sufficient dielectric strength (1-3 MV/cm) that switching and saturation occurred whenever six or more monolayers of NTCDI were deposited. The OSC layers were transparent, were switched below 1V, and showed promising radiation stability. For the thinnest

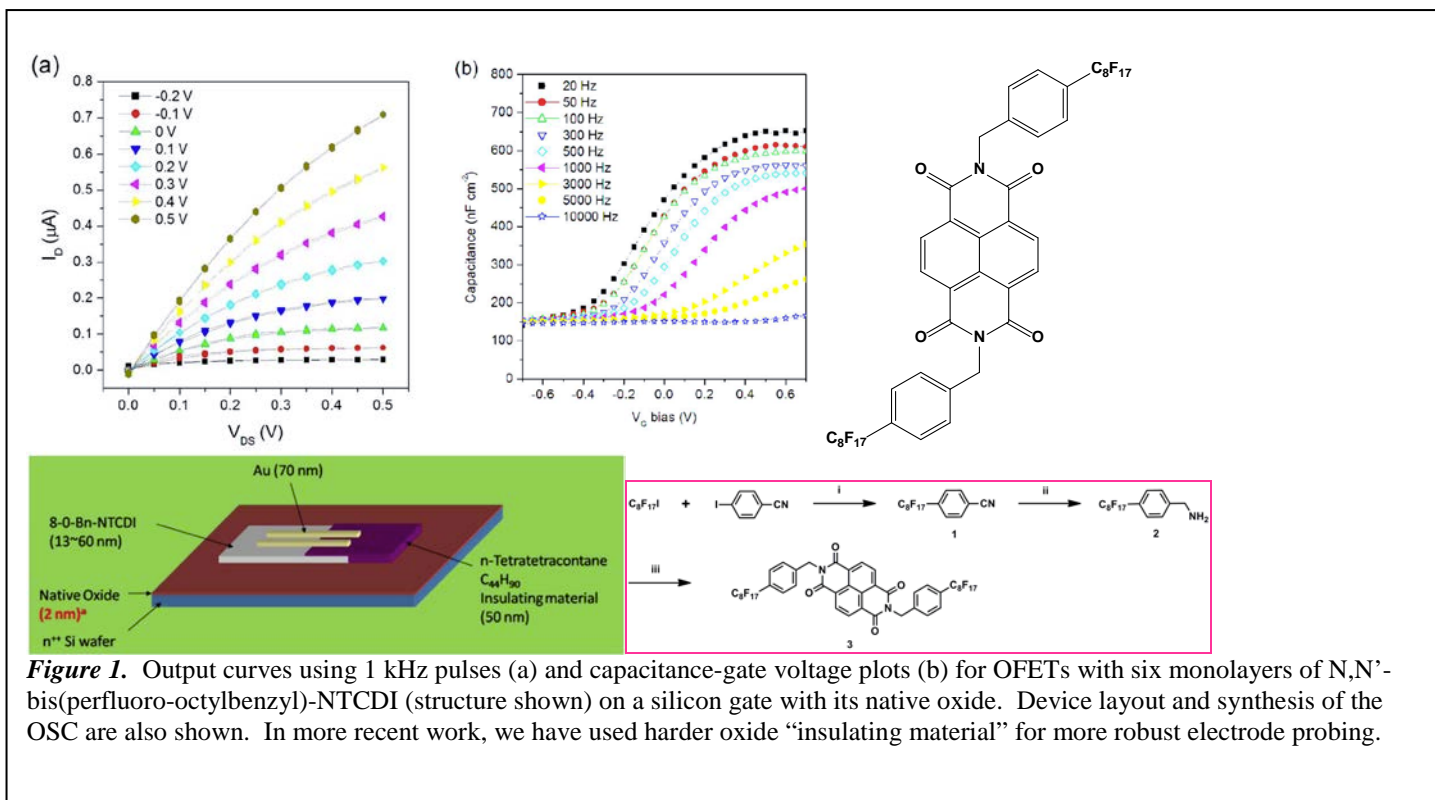
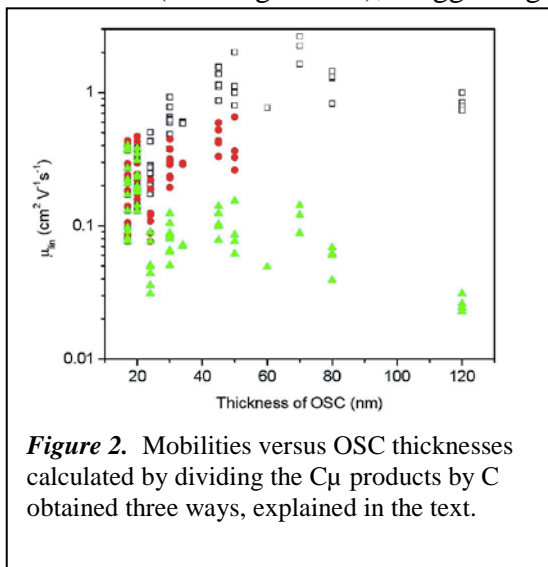


Figure 1. Output curves using 1 kHz pulses (a) and capacitance-gate voltage plots (b) for OFETs with six monolayers of N,N'-bis(perfluoro-octylbenzyl)-NTCDI (structure shown) on a silicon gate with its native oxide. Device layout and synthesis of the OSC are also shown. In more recent work, we have used harder oxide “insulating material” for more robust electrode probing.

NTCDI layers, the sheet transconductance (gate capacitance per unit area times the mobility, C_{μ} , obtained by fitting to the standard equation for FET drain current in saturation, $I_d = (WC\mu/2L)(V_g - V_t)^2$, C being capacitance per unit area, W/L the width/length ratio, and V_g and V_t the gate and threshold voltages, respectively) was >100 nS/V, *two orders of magnitude higher than typical thick-oxide OFETs and among the highest reported for any OFET*. Independent measurement of frequency-dependent capacitance showed that for the thinnest layers, the total capacitance equaled the sum of the oxide and one side chain capacitance in series. For thicker films, the capacitance was generally lower, indicating contributions from additional NTCDI layers. A two-segment N-side chain, the perfluoro-octylbenzyl of the Figure 1 structure or alternatively perfluoro-octylethylbenzyl, worked better for this purpose than the all-alkyl perfluoro-octylpropyl side chain.

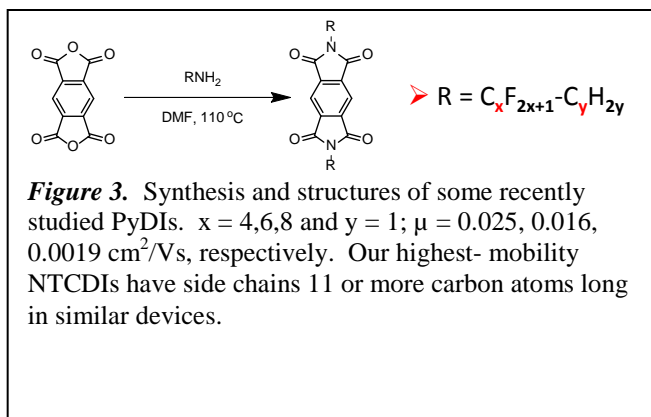
In the last ten years, many groups have studied high- ϵ dielectric layers in order to scale down dimensions and decrease operating voltages of OFETs relative to those using Si-SiO₂ technology.² They used very thin amorphous polymers³, monolayer-treated⁴⁻⁶ or polymer-treated inorganic dielectrics⁷, polymer electrolyte dielectrics⁸, and high k inorganic dielectrics.⁹ While attempts have been made to produce OFETs from single layers of molecules that included both a dielectric side chain and a conjugated subunit^{10,11}, the work reported here was the first demonstration of OSC molecular segments within a multilayer film contributing to gate capacitance, acting substantially as gate materials and avoiding the need for an independent dielectric deposition step.

An additional and profound observation was that μ calculated by dividing the $C\mu$ products by independently measured C depended on the frequency at which C and I_d were measured. C itself increased as frequency decreased (see Figure 1b), suggesting that times approaching one second were needed for complete



equilibration of charge distributions in this nonionic system. It should be noted that elsewhere, “mobility” values are rarely reported with any time dependence, and calculations of μ are generally based on C values taken at much higher frequency than the OFET output data. $C\mu$ products that we determined from I_d measured with 1-kHz pulses led to μ consistent with charges moving laterally in layers well above the gate. Figure 2 shows that μ (red circles) calculated from $C\mu$ products obtained from output curves at 1 kHz, divided by C measured independently at 1 kHz, were closer to μ (grey open squares) calculated by dividing $C\mu$ by a theoretical multilayer gate capacitance than to μ (green triangles) divided by the theoretical single layer C . We verified that contact resistance did not control I_d . The grain structure was highly two-dimensional, so μ did not decrease with L and therefore was probably not dominated by grain boundaries.

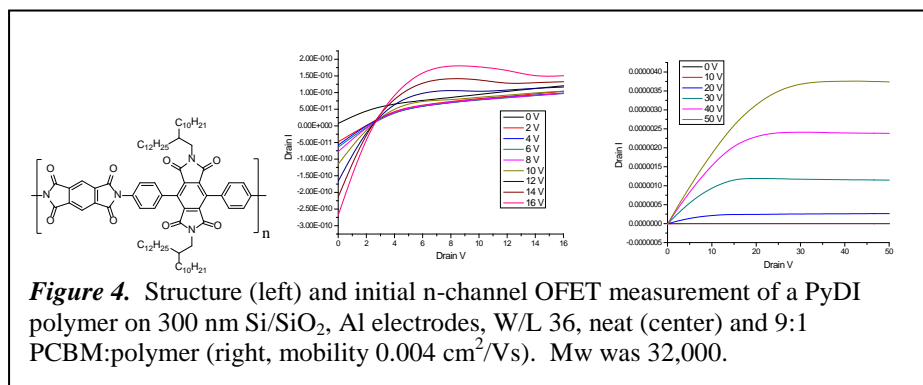
The dependence of μ on the vertical level in a two-dimensional grain or film has never been addressed experimentally. Two major theoretical studies have predicted a distribution of gate-induced charge carriers among various OSC layers above a gate. Horowitz¹² proposed that carriers would be distributed according to the thermodynamic equilibrium governed by the limits of how many charge carriers can reside on individual molecules, and how many can be confined in individual layers, in the case of layered OSC OFETs. This proposal is somewhat different from a model by deLeeuw for amorphous OFETs¹³ in which carriers would be locally distributed according to Poisson’s equation without as severe a geometric restriction. Horowitz makes the counterintuitive prediction that μ would increase for lower gate fields, where charges are farther from a trap-laden dielectric-OSC interface, a prediction for which this work is the first experimental verification. Most other prior work in this field is based on the assumption that μ increases with gate field as traps are progressively filled. An important scientific question to be answered in work of this proposal is whether the superior μ is because of better packing or fewer electronic traps in the upper layers relative to layers at the interface.



Other wide bandgap organic semiconductors. To minimize leakage current and create the dielectric-semiconductor hybrid structures of this proposal, it will be desirable to use OSCs with the maximum carrier energy that allows low contact resistance and environmental stability. Transparency is another desirable attribute. Because the ongoing project was designed with emphasis on n-channel OSCs, the NTCDI structure was emphasized, on which numerous high-electron-mobility semiconductors are based.¹⁴⁻¹⁶ In recent work, the even higher HOMO-LUMO gap (“bandgap”) pyromellitic diimide (PyDI) subunit has been shown to give reasonable mobilities.¹⁷

Results from seven different side chains suggest that optimal chain lengths for PyDIs are shorter than those of NTCDIs (Figure 3). Because of the higher electron energy in PyDIs and the decreased intermolecular overlap, μ is an order of magnitude lower than for NTCDIs.

The first hint of field-effect electron mobility (10^{-4} cm²/Vs) in such a polymer (Figure 4) and substantial μ from its blends with PCBM were observed. The polymer is rich in PyDI groups, but has a nonplanar main chain, side chains designed for larger fused rings¹⁸⁻²⁰, and high source to channel resistance, so great improvements can be anticipated, especially from planarization of the main chain²¹. The very possibility of n-OFETs from PyDI



OSCs had never been considered before, and their ready availability, ease of processing, transparency, and chemical/thermal stability make them attractive materials.

An important tool to enable the direct mapping of interfacial voltages at various device interfaces is scanning Kelvin probe microscopy (SKPM) (Figure 5). This enables

measurement of surface potentials versus position across pn junctions and gate dielectric-semiconductor boundaries.²² A major achievement of this effort was the fabrication of lateral analogs of normally vertical devices and observation of electric fields that control I-V relationships, monitoring of barrier voltages at the pn junction, while the device was operating.

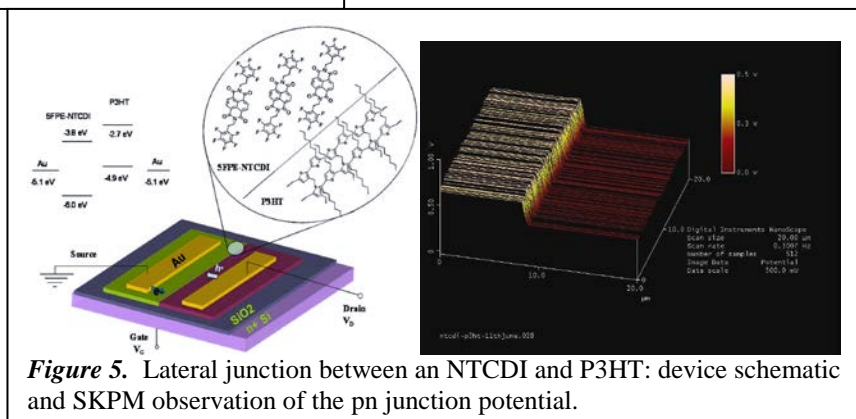


Figure 5. Lateral junction between an NTCDI and P3HT: device schematic and SKPM observation of the pn junction potential.

- 1 B. J. Jung, J. F. M. Hardigree, B. M. Dhar, T. J. Dawidczyk, J. Sun, K. C. See, and H. E. Katz, *Naphthalenetetracarboxylic Diimide Layer-Based Transistors with Nanometer Oxide and Side Chain Dielectrics Operating below One Volt*, *ACS Nano* **5**, 2723 (2011).
- 2 R. P. Ortiz, A. Facchetti, and T. J. Marks, *High-k Organic, Inorganic, and Hybrid Dielectrics for Low-Voltage Organic Field-Effect Transistors*, *Chemical Reviews* **110**, 205 (2010).
- 3 L. Wang, M. H. Yoon, G. Lu, Y. Yang, A. Facchetti, and T. J. Marks, *High-performance transparent inorganic-organic hybrid thin-film n-type transistors*, *Nature Materials* **5**, 893 (2006).
- 4 O. Acton, G. Ting, H. Ma, J. W. Ka, H. L. Yip, N. M. Tucker, and A. K. Y. Jen, *pi-sigma-Phosphonic Acid Organic Monolayer/Sol-Gel Hafnium Oxide Hybrid Dielectrics for Low-Voltage Organic Transistors*, *Advanced Materials* **20**, 3697 (2008).
- 5 M. Halik, H. Klauk, U. Zschieschang, G. Schmid, C. Dehm, M. Schutz, S. Maisch, F. Effenberger, M. Brunnbauer, and F. Stellacci, *Low-voltage organic transistors with an amorphous molecular gate dielectric*, *Nature* **431**, 963 (2004).
- 6 H. Klauk, U. Zschieschang, J. Pflaum, and M. Halik, *Ultralow-power organic complementary circuits*, *Nature* **445**, 745 (2007).
- 7 L. A. Majewski, R. Schroeder, and M. Grell, *One volt organic transistor*, *Advanced Materials* **17**, 192 (2005).
- 8 M. J. Panzer and C. D. Frisbie, *Polymer electrolyte gate dielectric reveals finite windows of high conductivity in organic thin film transistors at high charge carrier densities*, *Journal of the American Chemical Society* **127**, 6960 (2005).
- 9 B. N. Pal, B. M. Dhar, K. C. See, and H. E. Katz, *Solution-deposited sodium beta-alumina gate dielectrics for low-voltage and transparent field-effect transistors*, *Nature Materials* **8**, 898 (2009).
- 10 S. G. J. Mathijssen, E. C. P. Smits, P. A. van Hal, H. J. Wondergem, S. A. Ponomarenko, A. Moser, R. Resel, P. A. Bobbert, M. Kemerink, R. A. J. Janssen, and D. M. de Leeuw, *Monolayer coverage and channel length set the mobility in self-assembled monolayer field-effect transistors*, *Nature Nanotechnology* **4**, 674 (2009).
- 11 M. Mottaghi, P. Lang, F. Rodriguez, A. Rumyantseva, A. Yassar, G. Horowitz, S. Lenfant, D. Tondelier, and D. Vuillaume, *Low-operating-voltage organic transistors made of bifunctional self-assembled monolayers*, *Advanced Functional Materials* **17**, 597 (2007).
- 12 G. Horowitz, *Organic thin film transistors: From theory to real devices*, *Journal of Materials Research* **19**, 1946 (2004).
- 13 C. Tanase, E. J. Meijer, P. W. M. Blom, and D. M. de Leeuw, *Local charge carrier mobility in disordered organic field-effect transistors*, *Organic Electronics* **4**, 33 (2003).
- 14 J. E. Anthony, A. Facchetti, M. Heeney, S. R. Marder, and X. W. Zhan, *n-Type Organic Semiconductors in Organic Electronics*, *Advanced Materials* **22**, 3876 (2010).

- 15 B. J. Jung, N. J. Tremblay, M. L. Yeh, and H. E. Katz, *Molecular Design and Synthetic Approaches to Electron-Transporting Organic Transistor Semiconductors*, *Chemistry of Materials* **23**, 568 (2011).
- 16 X. W. Zhan, A. Facchetti, S. Barlow, T. J. Marks, M. A. Ratner, M. R. Wasielewski, and S. R. Marder, *Rylene and Related Diimides for Organic Electronics*, *Advanced Materials* **23**, 268 (2011).
- 17 Q. D. Zheng, J. Huang, A. Sarjeant, and H. E. Katz, *Pyromellitic Diimides: Minimal Cores for High Mobility n-Channel Transistor Semiconductors*, *Journal of the American Chemical Society* **130**, 14410 (2008).
- 18 Z. H. Chen, Y. Zheng, H. Yan, and A. Facchetti, *Naphthalenedicarboximide- vs Perylenedicarboximide-Based Copolymers. Synthesis and Semiconducting Properties in Bottom-Gate N-Channel Organic Transistors*, *Journal of the American Chemical Society* **131**, 8 (2009).
- 19 H. Yan, Z. H. Chen, Y. Zheng, C. Newman, J. R. Quinn, F. Dotz, M. Kastler, and A. Facchetti, *A high-mobility electron-transporting polymer for printed transistors*, *Nature* **457**, 679 (2009).
- 20 X. W. Zhan, Z. A. Tan, E. J. Zhou, Y. F. Li, R. Misra, A. Grant, B. Domercq, X. H. Zhang, Z. S. An, X. Zhang, S. Barlow, B. Kippelen, and S. R. Marder, *Copolymers of perylene diimide with dithienothiophene and dithienopyrrole as electron-transport materials for all-polymer solar cells and field-effect transistors*, *Journal of Materials Chemistry* **19**, 5794 (2009).
- 21 M. M. Durban, P. D. Kazarinoff, Y. Segawa, and C. K. Luscombe, *Synthesis and Characterization of Solution-Processable Ladderized n-type Naphthalene Bisimide Copolymers for OFET Applications* *Macromolecules* **44**, 4721 (2011).
- 22 B. M. Dhar, G. S. Kini, G. Q. Xia, B. J. Jung, N. Markovic, and H. E. Katz, *Field-effect-tuned lateral organic diodes*, *Proceedings of the National Academy of Sciences of the United States of America* **107**, 3972 (2010).